

Comparison of Valid Ocean Observations Between MODIS Terra and Aqua Over the Global Oceans

Lian Feng and Chuanmin Hu

Abstract—Ocean color satellite missions to measure the biophysical and geochemical properties of the surface ocean need to consider not only the spectral and spatial requirements of the sensors but also the satellite overpass time to maximize valid observations. The valid observations are impacted not only by cloud cover but also by other perturbations such as sun glint and stray light. Using Level-3 global composites of three ocean products (chlorophyll a or Chl-a, normalized fluorescence line height or nFLH, and sea surface temperature or SST), the daily percentage valid observations (DPVOs) over the global oceans were calculated, from which the differences between MODIS Aqua (afternoon pass) and MODIS Terra (morning pass) have been analyzed. For all three products, Aqua shows more valid observations than Terra over the Southern Ocean, the ocean near Peru and Chile, and the ocean around Angola and Namibia, with relatively >30% more valid observations in boreal winter months due to lower cloud coverage in the afternoon. In contrast, more than 20% of valid Chl-a and nFLH observations are obtained by Terra in the North Indian Ocean, and 10%–30% more valid observations by Terra are also found for the Equatorial Pacific and Atlantic oceans. These can be possibly linked to the lower presence of sun glint for Terra. Compared with Chl-a and nFLH, SST retrievals are more tolerant to sun glint and other perturbation factors, leading to much higher DPVOs. The implications of these findings to future satellite mission design and field campaigns are also discussed.

Index Terms—Aqua, chlorophyll-a (Chl-a), cloud cover, high quality, normalized fluorescence line height (nFLH), ocean color, remote sensing, sea surface temperature (SST), sun glint, Terra, valid observation.

I. INTRODUCTION

ONE primary advantage of satellite remote sensing is its synoptic and repeated measurements over the Earth. For example, with their wide swaths (~ 2330 km), each of the Moderate Resolution Imaging Spectroradiometers (MODIS) on board the polar orbiting satellites Terra (1999 to present, 10:30 equatorial crossing time) and Aqua (2002 to present, 13:30 equatorial crossing time) can cover the entire Earth every two days [1]. Over high-latitude regions, the satellite measurements are more frequent, and sometimes, multiple visits per day can be also achieved. The most recent Visible Infrared Imaging

Manuscript received July 20, 2015; revised September 21, 2015; accepted September 25, 2015. Date of publication November 3, 2015; date of current version February 24, 2016. This work was supported in part by the NASA Ocean Biology and Biogeochemistry Program and in part by a grant to support NASA's Geostationary Coastal and Air Pollution Events mission design.

The authors are with the College of Marine Science, University of South Florida, St. Petersburg, FL 33701 USA (e-mail: lianfeng619@gmail.com).

Color versions of one or more of the figures in this paper are available online at <http://ieeexplore.ieee.org>.

Digital Object Identifier 10.1109/TGRS.2015.2483500

Radiometer Suite (2011 to present) has a swath width of 3000 km, providing more synoptic observation than MODIS [2], [3]. Together with other satellite ocean color missions, they have provided unprecedented information to study the biophysical and biogeochemical properties and processes of the surface oceans in both global and regional scales.

However, due to the presence of unfavorable measurement conditions such as clouds, sun glint, stray light, or extreme solar/viewing geometry [4], in reality, the coverage of valid observations is much less than once every two days. For example, Maritorena *et al.* [5] showed that, on average, valid MODIS Aqua retrievals over the global oceans were only 12% per day. In some regions, there can be less than one valid observation per month due to persistent cloud cover. Such limited observations pose a challenge in composing seamless time series to observe ocean changes in both short term and long term. For example, Barnes and Hu [2] showed that only when the number of valid observations exceeded 10 per month did MODIS and the Sea-viewing Wide Field-of-view Sensor (SeaWiFS) agreed to within 10% in their monthly mean chlorophyll-a (Chl-a) data product for any 0.25° gridded locations in the Gulf of Mexico.

While the increased valid observations can be achieved through multisensor merging (e.g., [5]) or a geostationary satellite such as the Geostationary Ocean Color Imager (2010 to present; see [6]) or the planned Geostationary Coastal and Air Pollution Events (GEO-CAPE) [7], it is desirable to know the optimal observation time window for polar orbiters in order to better plan future satellite missions. In particular, given the limited resources available on a geostationary satellite and the competing demands to measure different regions, it is impossible for GEO-CAPE to measure all coastal waters at hourly frequency within its field of view (FOV) at the planned 375-m nadir resolution on a routine basis. It is therefore also required to know when is the best season (or month) and when is the best observation time during a day to measure a certain region.

However, such a question cannot be easily addressed for two reasons. First, even if cloud statistics is available from either MODIS (MOD08 for Terra and MYD08 for Aqua) [8]–[10] or Geostationary Operational Environmental Satellite system [11], the statistics of high-quality ocean color data retrievals could be different because cloud cover is not the only factor that affects data quality. For example, sun glint contamination is another important factor that influences the quality of Chl-a and nFLH retrievals, but sun glint is independent of clouds [12]. Second, when existing sensors with different equatorial crossing times are compared, the results may be biased due to their different swath widths and band settings. Fortunately, statistics of valid

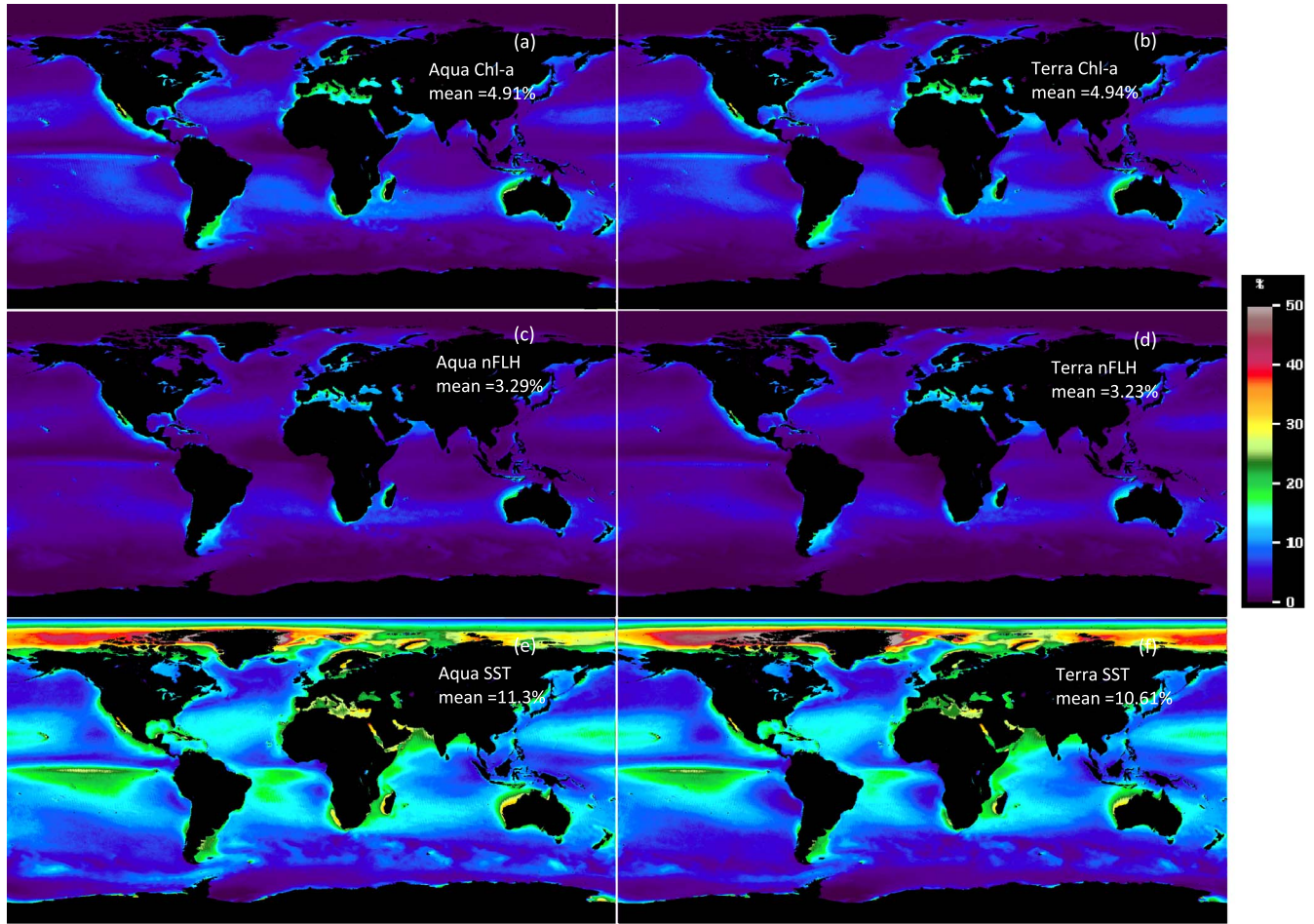


Fig. 1. Mean DPVOs for Chl-a, nFLH, and SST during 2003–2014 for MODIS Terra and MODIS Aqua.

data retrievals for two MODIS instruments with identical swath widths and band settings have been generated by the NASA Ocean Biology Processing Group (OBPG), which provide the basis to address the aforementioned questions.

Thus, the objectives of this analysis are to do the following.

- 1) compare valid observations between MODIS Aqua and MODIS Terra in a statistical meaningful way to determine if one sensor can provide more valid observations than the other and, if so, when and where;
- 2) compare valid observations between different data products for the same sensor;
- 3) provide recommendations for future satellite missions on equatorial crossing time.

II. DATA AND METHODS

Monthly global binned MODIS Level-3 standard mapped image (SMI) data at 4-km resolution between January 2003 and December 2014 were downloaded from the NASA Goddard Space Flight Center (GSFC). The data include Chl-a ($\text{mg} \cdot \text{m}^{-3}$), normalized fluorescence line height (nFLH, $\text{mW} \cdot \text{cm}^{-2} \cdot \mu\text{m}^{-1} \cdot \text{sr}^{-1}$), and sea surface temperature (SST, $^{\circ}\text{C}$). The selection of these three products was based on their importance in addressing ocean science questions.

Chl-a is a critical parameter in ocean biology and biogeochemistry, whereas SST plays a key role in observing physical processes (e.g., heat flux) and climate variability. nFLH is a measure of solar-stimulated phytoplankton fluorescence that has been used to study global ocean phytoplankton physiology [13] and coastal algal blooms [14], [15].

For each gridded cell ($4.6 \text{ km} \times 4.6 \text{ km}$), the mean, standard deviation, and variance values of the parameter of interest are available for analysis. In addition, the number of valid retrievals (i.e., observations) of that parameter for each cell is also available. Here, the term “valid” means that the Level-2 data used in composing the Level-3 data are not associated with any of the quality control flags. These flags include (see [2, Table I]) the following: atmospheric correction failure, land, high glint, high radiance, high satellite zenith angle, straylight, cloud/ice, high solar zenith angle, low water-leaving radiance, Chl-a algorithm failure, navigation warning, maximum iteration exceeded, Chl-a algorithm warning, atmospheric correction warning, and navigation failure. These flags were used to screen bad or low-quality data when generating daily, eight-day, or monthly composites by the NASA OBPG [16]. Each product has its own flag set due to their different requirements on the measurement conditions. The flag requirement on nFLH is more conservative

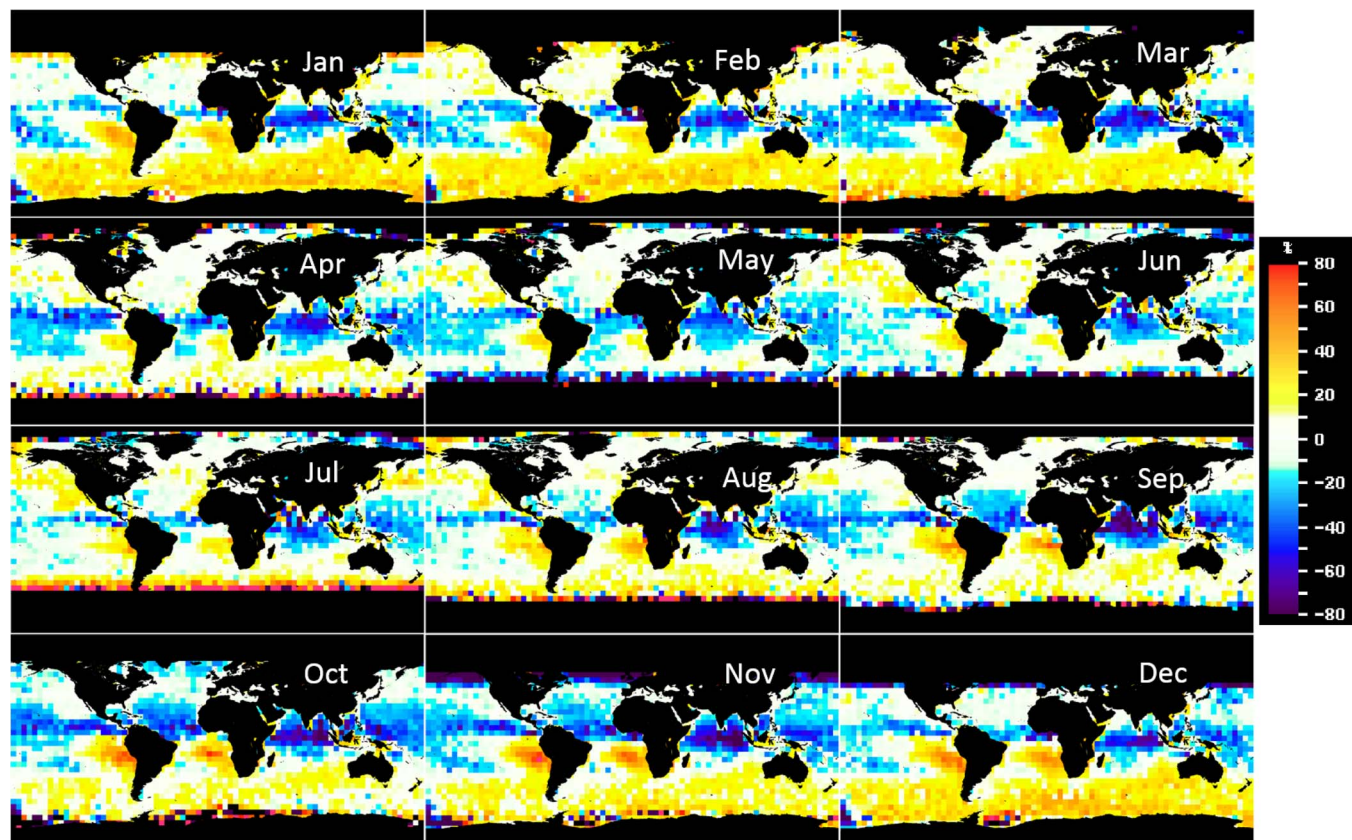


Fig. 2. Relative differences between DPVOs of Chl-a between MODIS Aqua and Terra for the 12 climatological months. The relative difference is expressed as $(\text{Aqua} - \text{Terra})/\text{Aqua} \times 100\%$.

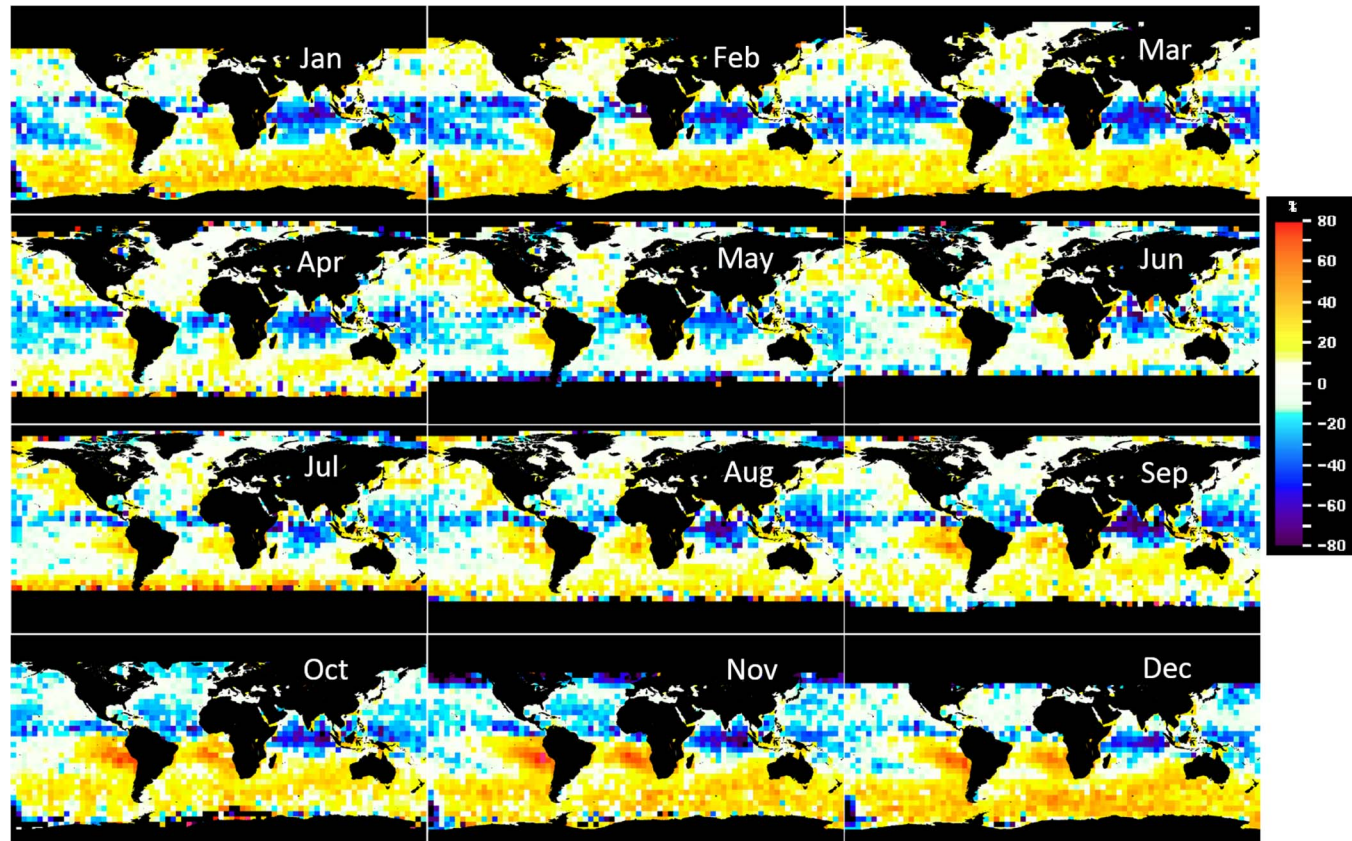


Fig. 3. Relative differences between DPVOs of nFLH between MODIS Aqua and Terra for the 12 climatological months. The relative difference is expressed as $(\text{Aqua} - \text{Terra})/\text{Aqua} \times 100\%$.

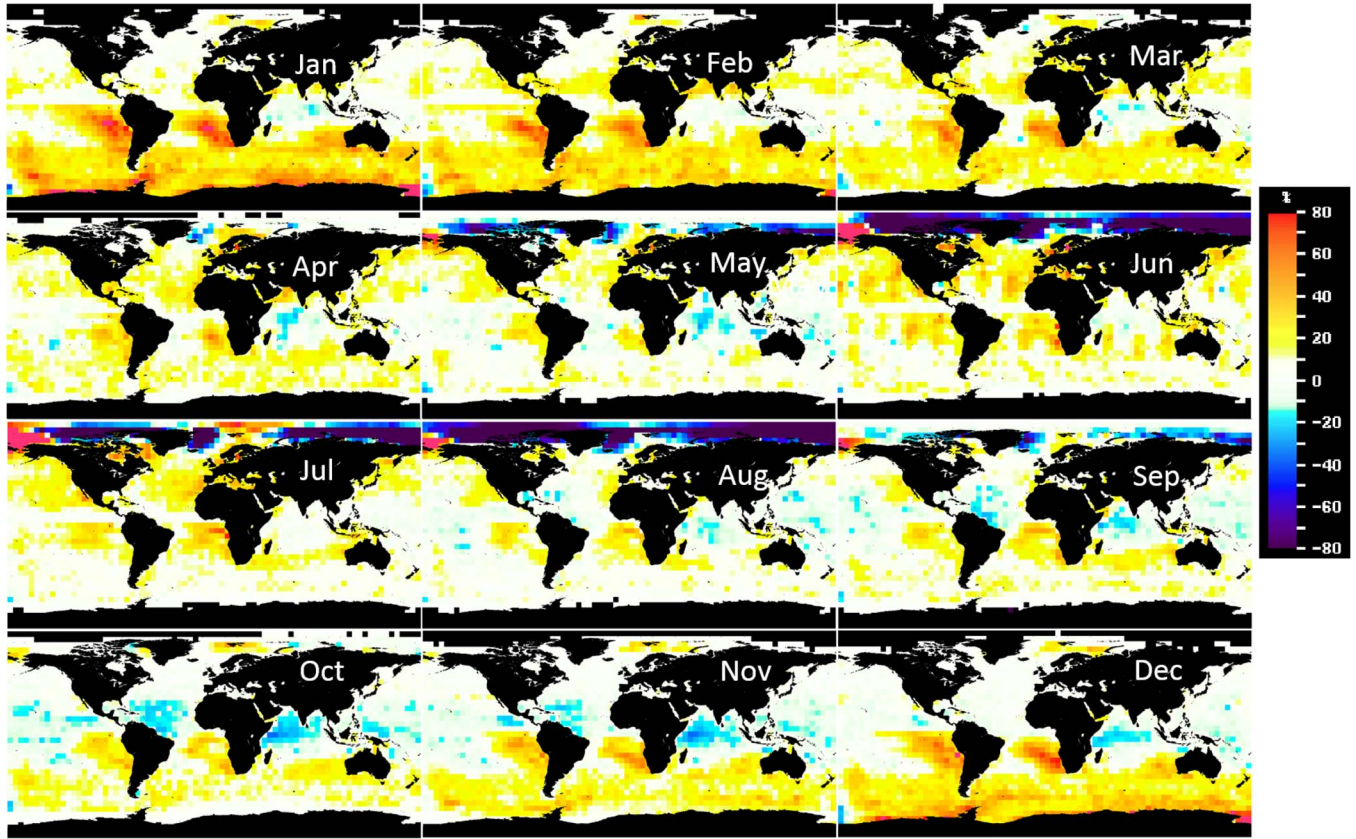


Fig. 4. Relative differences between DPVOs of SST between MODIS Aqua and Terra for the 12 climatological months. The relative difference is expressed as $(\text{Aqua} - \text{Terra})/\text{Aqua} \times 100\%$.

than on Chl-a, with two additional flags of “MODGLINT” and “PRODWARN” being used. The MODGLINT flag represents moderate sun glint contamination (glint reflectance between 0.005 and 0.01 sr^{-1}), and PRODWARN represents diffuse attenuation (K_{490}) out of a meaningful range. A separate flag set is used for generating the SST products, where the highest data quality (0 and 1 from the “sst_qual” flag) was used in generating global composite data.

The number of valid observations for each grid cell (N_V) is the focus of this analysis. A key variable derived from N_V is the daily percentage valid observations (DPVOs), which is defined as

$$\text{DPVO} = N_V / (4.6 \times 4.6) / \# \text{ of days during a month} \times 100\% \quad (1)$$

where 4.6×4.6 accounts for the number of 1-km pixels in the 4.6×4.6 km grid cell. For example, a DPVO of 25% means that, for every 1-km location within that grid cell, the chance of having valid data for any given day of that month is 25%. To minimize the effects of patchiness to observe the spatially coherent patterns, the 4.6-km data were further aggregated into $\sim 4.6^\circ \times 4.6^\circ$ cells, where the value of each cell was the mean of the 110×110 4.6-km grid cells. The DPVO monthly data between 2003 and 2014 were used to estimate the monthly climatological statistics of Chl-a, nFLH, and SST for both Terra and Aqua (denoted by Γ_{Terra} and Γ_{Aqua} , respectively), from which the mean DPVO for the entire observation period

was also estimated for each product. Then, the difference between Terra and Aqua for each climatological month was calculated in terms of both absolute ($\Gamma_{\text{Aqua}} - \Gamma_{\text{Terra}}$) and relative ($(\Gamma_{\text{Aqua}} - \Gamma_{\text{Terra}})/\Gamma_{\text{Aqua}} \times 100\%$) differences, based on which the mean differences during the 12-year period were also obtained.

Additionally, the DPVO differences between different data products for the same sensor were calculated between Chl-a and nFLH and between SST and Chl-a. Such differences were averaged for four quarters, with Quarter 1 starting in January and ending in March and so on. The DPVO differences between these products can be used to evaluate how the DPVOs of different products can be affected by noncloud factors.

Monthly cloud fraction data (MOD08 for Terra and MYD08 for Aqua, respectively) for daytime observations were obtained from the Geospatial Interactive Online Visualization And aNalysis Infrastructure of the Goddard Earth Sciences Data and Information Services Center [17]. The data were used to understand the DPVO differences between Terra and Aqua. Cloud fraction was derived from the MODIS cloud mask products (MOD35 for Terra and MYD35 for Aqua), which is defined as the number of cloudy and probably cloudy pixels divided by the total number of pixels in each gridded cell [8]. The Level-3 cloud fraction (C_f) data had a $1^\circ \times 1^\circ$ grid on an equal-angle projection. For each grid, the noncloud fraction was calculated as $1 - C_f$, which can be also interpreted as noncloud probability.

To further diagnose which noncloud factors also led to failures in valid data retrievals, MODIS Level-2 products for both MODIS Aqua (133 granules) and MODIS Terra (135 granules) over the Indian Ocean for January 2006 were also downloaded from the NASA GSFC. The cloud coverage for each granule was first determined using the l2_flags (pixels associated with bit 10 in l2_flags were deemed as clouds). Here, the technical definition of clouds is when the Rayleigh-corrected reflectance in the near-infrared band (869 nm), after removal of the glint reflectance, exceeds 2.7%. Then, the monthly mean noncloud coverages for both MODIS instruments were estimated based on the cloud masks determined by the l2_flags, which were then used to compare with those determined from the cloud fraction products (i.e., $1 - C_f$) from MOD35.

To evaluate the potential impact of sun glint, monthly global binned SeaWiFS Level-3 SMI Chl-a data at 9-km resolution for the months of January and June 2003 were downloaded from the NASA GSFC. SeaWiFS tilts away from nadir by about 22° , thus could avoid most of the sun glint. A comparison with the corresponding MODIS months could reveal the potential sun glint effects on MODIS DPVOs.

III. RESULTS

A. DPVO Differences Between the Two MODIS Instruments

Fig. 1 shows the mean DPVOs of Chl-a, nFLH, and SST from the two MODIS instruments for 2003–2014. Generally, the DPVOs for Chl-a and nFLH are less than 20% and 15% for most locations, and the global mean DPVOs are only $\sim 4.9\%$ for Chl-a and 3.2% for nFLH. In contrast, SST shows much higher DPVOs, with global means around 11% and higher values of $\sim 20\%$ in major ocean gyres and $> 40\%$ in the Arctic Ocean [see Fig. 1(e) and (f)]. Note that, for high-latitude scenes, MODIS could provide several measurements in a day, which partly explains the high DPVOs for SST over the Arctic Ocean; however, DPVOs for Chl-a and nFLH over the same region are still very low.

The relative differences in DPVOs of Chl-a between MODIS Aqua and MODIS Terra are illustrated in Fig. 2, with warm colors representing higher DPVOs from MODIS Aqua. Both the spatial distribution patterns and their seasonality can be visualized from these difference images. In general, Terra shows higher DPVOs near the equatorial zones for all months, whereas Aqua shows more valid observations in the Southern Ocean, particularly during the boreal winter months. Additionally, two subregions show more valid observations from Aqua for all months; these are located in the oceans near Peru and Chile of South America (denoted by PC in the following text) and Angola and Namibia (denoted by AN in the following text) of South Africa. Furthermore, the relative differences in DPVOs of nFLH between Terra and Aqua show spatial patterns and seasonality similar to those of Chl-a (see Fig. 3).

The relative difference patterns in DPVOs of SST across the two sensors appear different from those of Chl-a and nFLH (see Fig. 4). For most oceans, DPVOs from the two sensors are comparable (white color), particularly in some boreal summer and autumn months. For other regions, Aqua has higher DPVOs

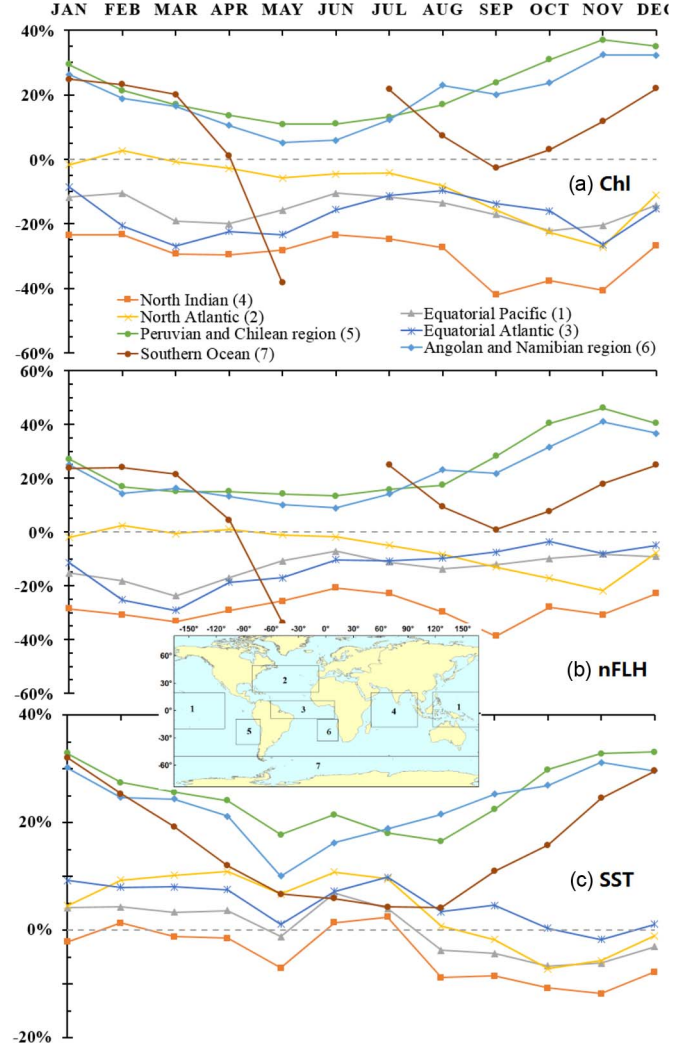


Fig. 5. Mean relative differences of DPVOs of (a) Chl-a, (b) nFLH, and (c) SST between MODIS Aqua and MODIS Terra for several regions for the 12 climatological months. No Chl-a or nFLH data are available in the polar night period in June for the Southern Ocean. The relative difference is expressed as $(\text{Aqua} - \text{Terra})/\text{Aqua} \times 100\%$.

than Terra, particularly for the Southern Ocean during the boreal winter months. Furthermore, higher DPVOs from Aqua are observed for the PC and AN oceans in all 12 months and for the north Atlantic and Pacific Oceans in some months. For the Arctic Ocean, lower DPVOs are found from Aqua between May and September.

To facilitate visualizing the relative differences between the two MODIS instruments, Fig. 5 shows the mean relative differences of several regions for the 12 climatological months. Similar to Fig. 2, the tropical and subtropical regions show lower DPVOs of Chl-a from Aqua [see Fig. 5(a)]. For the North Indian Ocean, Aqua shows at least 20% less Chl-a retrievals relative to Terra for all months and $\sim 40\%$ less Chl-a retrievals during boreal autumn months (September to November). For the Equatorial Pacific and Atlantic, Aqua shows 30%–10% less Chl-a retrievals for different months. In contrast, more valid retrievals are found from Aqua than from Terra for the PC and AN regions during all months, with Aqua being $> 30\%$ higher than Terra during the boreal winter months (December to

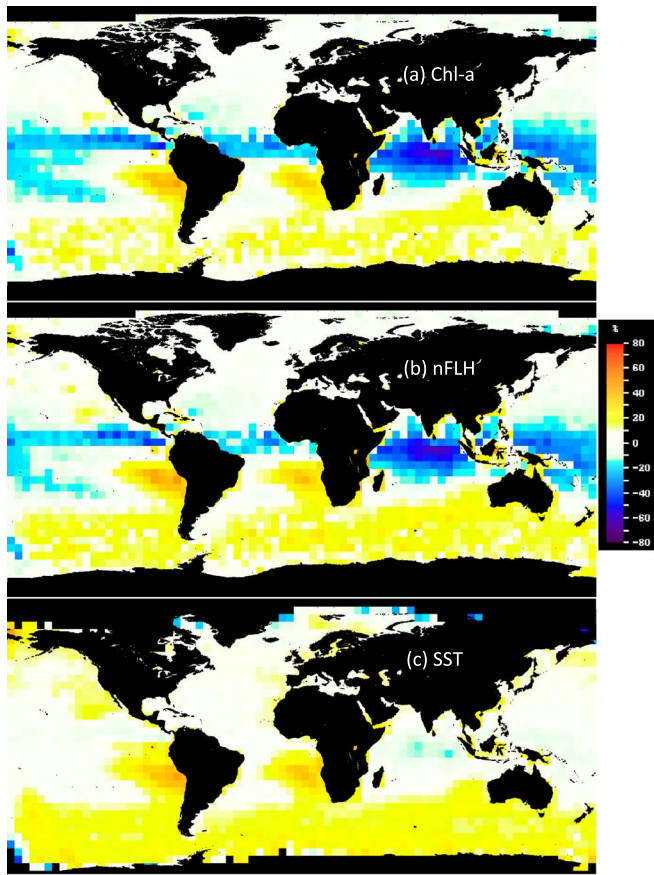


Fig. 6. Mean relative differences of DPVOs of Chl-a, nFLH, and SST between MODIS Aqua and MODIS Terra for the 12 climatology months. The relative difference is expressed as $(\text{Aqua} - \text{Terra})/\text{Aqua} \times 100\%$.

February). On the other hand, the relative differences fluctuate for the Southern Ocean, with more months showing higher Aqua retrievals. The mean relative differences between Aqua and Terra for DPVOs of nFLH are demonstrated in Fig. 5(b), whose patterns for the selected regions appear very similar to those of Chl-a.

The mean relative differences between Aqua and Terra for valid SST retrievals for all selected regions are generally positive, except for the North Indian Ocean, North Atlantic, Equatorial Pacific, and Equatorial Atlantic during certain months. Similar to Chl-a and nFLH, SST shows much lower DPVOs from Aqua than from Terra for all 12 months for the North Indian Ocean. In contrast, Aqua shows higher DPVOs than Terra in the other three regions (the Southern Ocean and PC and AN regions) for all 12 months, with their relative difference reaching $\sim 40\%$ during the boreal winter months.

The climatological annual mean relative differences (i.e., mean of the 12 climatological months) are shown in Fig. 6. Similar to the monthly differences, the spatial patterns of Chl-a and nFLH mimic each other, with higher DPVOs for Aqua over the Southern Ocean and the PC and AN regions. The tropical and subtropical oceans often show higher DPVOs from Terra than from Aqua. For SST, Aqua shows higher DPVOs over the Southern Ocean, North Atlantic, and the PC and AN regions; whereas slightly lower DPVOs are found from Aqua over the Northern Indian Ocean.

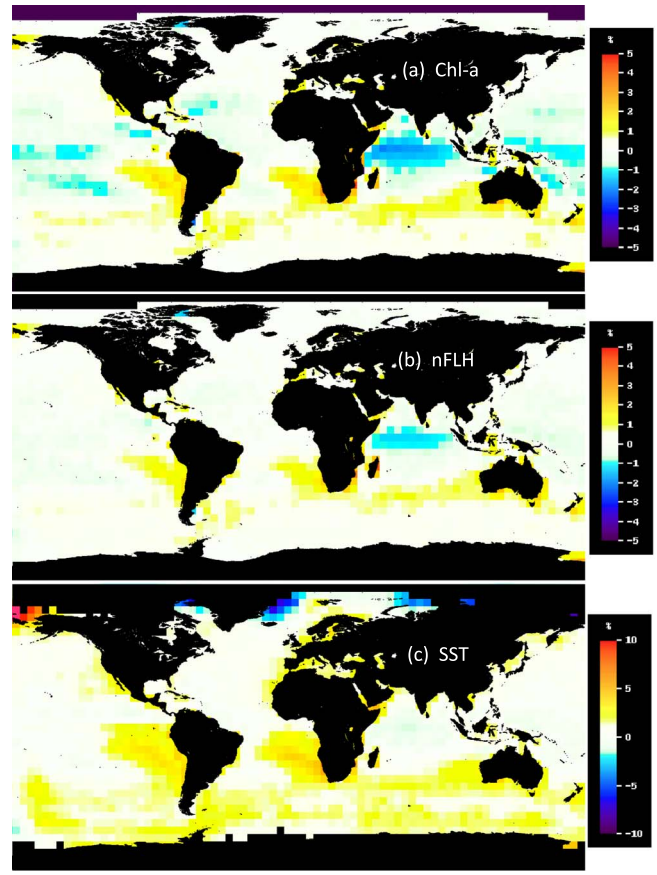


Fig. 7. Mean absolute differences of DPVOs of Chl-a, nFLH, and SST between MODIS Aqua and MODIS Terra for the 12 climatology months. The absolute difference is expressed as $(\text{Aqua} - \text{Terra})$.

Corresponding to the relative differences in Fig. 6, the absolute differences between DPVOs of Aqua and Terra for the three products are shown in Fig. 7. Such absolute differences are within 5% for Chl-a and nFLH and within 10% for SST. Compared with the spatial distribution patterns in the relative difference images, both positive and negative absolute differences for Chl-a and nFLH are less pronounced, with values for the tropical and subtropical oceans of Pacific and Atlantic being $< 1\%$ (light blue to white color). This is because the DPVOs for Chl-a and nFLH are very small (see Fig. 1), making the cross-sensor absolute differences even smaller. In contrast, the relative and absolute differences between Aqua and Terra for SST show similar spatial patterns, except for the Arctic Ocean.

B. DPVO Differences Between Different Products

Fig. 8 shows the mean relative differences of DPVOs between Chl-a and nFLH from MODIS Aqua, whereas the seasonal and spatial patterns for MODIS Terra are very similar and therefore not shown here. DPVOs of Chl-a are always higher than those of nFLH, as two additional quality control flags were used to screen nFLH data. Superimposed on the positive differences are the seasonal changes of the global distributions. Chl-a has much higher DPVOs than nFLH over the tropical and subtropical gyres, and this pattern is more significant in Quarters 2 and 3. For the Southern Ocean, while the two

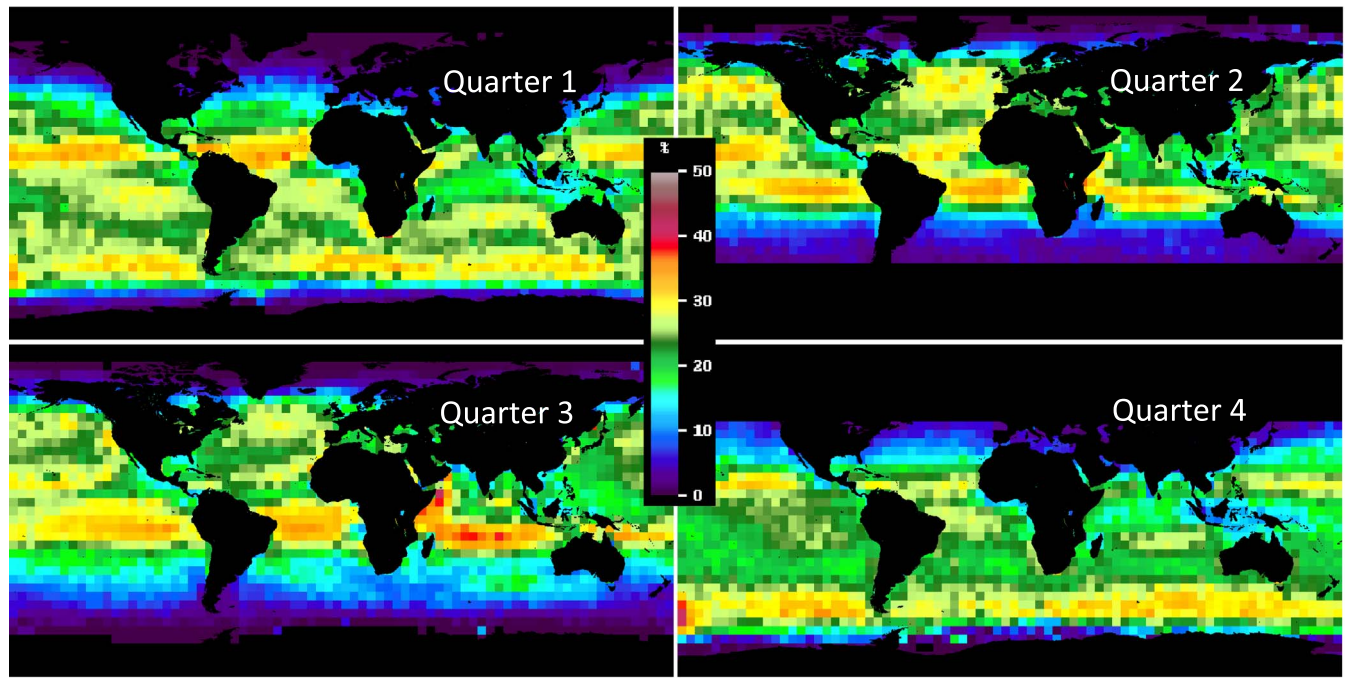


Fig. 8. Mean relative differences between DPVOs of Chl-a and nFLH from MODIS Aqua measurements. The relative difference is expressed as $(\text{Chl-a} - \text{nFLH}) / \text{Chl-a} \times 100\%$.

TABLE I
RELATIVE DIFFERENCES BETWEEN DPVOs OF CHL AND NFLH
AND BETWEEN DPVOs OF SST AND CHL FOR MODIS
AQUA AND MODIS TERRA. THE MEAN CONDITIONS
ARE SHOWN IN THE LAST ROW

| | Chl-nFLH | | SST-Chl | |
|----------|----------|-------|---------|-------|
| | Aqua | Terra | Aqua | Terra |
| Quarter1 | 32.9% | 31.9% | 55.8% | 52.7% |
| Quarter2 | 27.6% | 29.1% | 48.2% | 42.0% |
| Quarter3 | 29.7% | 31.0% | 49.9% | 48.0% |
| Quarter4 | 29.1% | 33.2% | 55.4% | 52.5% |
| Mean | 29.8% | 31.3% | 52.3% | 48.8% |

products have similar DPVOs in Quarters 2 and 3 (relative difference <10%), discernable higher DPVOs in Chl-a can be found in Quarters 1 and 4. On the other hand, no significant difference was found for the Arctic Ocean for all four quarters. Overall, global statistics in Table I reveal that the DPVOs for Chl-a are 27.6%–32.9% higher than the DPVOs for nFLH for the four quarters, with a mean of 29.8% for Aqua and a mean 31.3% for Terra.

Large relative differences between DPVOs for SST and Chl-a are also found (see Fig. 9). Clearly, SST has more valid retrievals than Chl-a. Specifically, the DPVOs of SST are considerably higher than the DPVOs of Chl-a for the tropical and subtropical oceans, particularly for the Equatorial Atlantic for all four quarters and for the Northern Indian Ocean for Quarter 3. Large differences are also observed over the Arctic Ocean for Quarters 2 and 3 and over the Antarctic Ocean for Quarters 1 and 4. In contrast, a large portion of the oceans in the Southern Hemisphere shows relatively small difference

between DPVOs of SST and Chl-a in Quarters 2 and 3. On average, the global oceans show ~50% higher DPVOs in SST than in Chl-a (see Table I).

IV. DISCUSSION

A. Factors Affecting DPVOs

From the global perspective, cloud coverage over the oceans is slightly higher for Terra than for Aqua [9]. However, more diurnal changes in cloud cover do occur in certain regions, leading to potentially significant differences of DPVOs between MODIS Terra and Aqua. To verify this potential cause, global cloud fraction products of the two MODIS instruments were examined.

Fig. 10 shows the mean relative differences of noncloud fraction between Aqua and Terra for the four quarters, estimated using the monthly cloud fraction products within the same period (January 2003 to December 2014). Clearly, the noncloud fraction of Aqua is higher than or at least equal to that of Terra over most of the global oceans, except for the high-latitude regions in certain quarters. In particular, Aqua shows consistently higher noncloud fraction in the PC and AN regions than Terra in every quarter (see Fig. 10), explaining the higher DPVOs for all three products from Aqua (see Figs. 5 and 6). Indeed, the PC and AN regions are well known for their marine stratocumulus clouds, which tend to thin out and burn off in the afternoon [9], [18]. Likewise, cloud coverage for Aqua over the Southern Ocean is lower than for Terra, particularly in Quarters 1 and 4, explaining the higher DPVOs from Aqua during these periods (see Fig. 5). Overall, the large positive differences in the DPVOs between Aqua and Terra in these regions (PC and AN regions and the Southern Ocean) can be well explained by

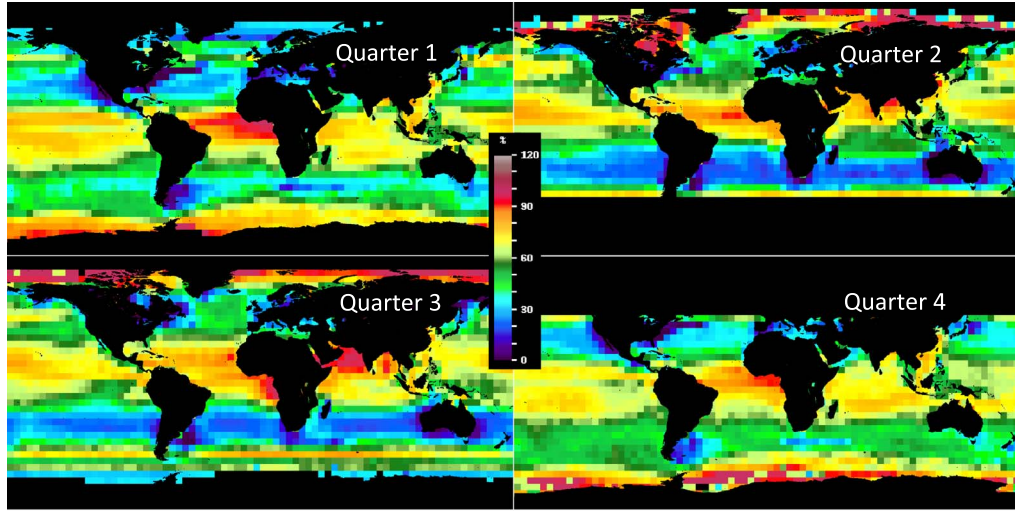


Fig. 9. Mean relative differences between DPVOs of SST and Chl-a from MODIS Aqua measurements. The relative difference is expressed as $(\text{SST} - \text{Chl-a})/\text{SST} \times 100\%$.

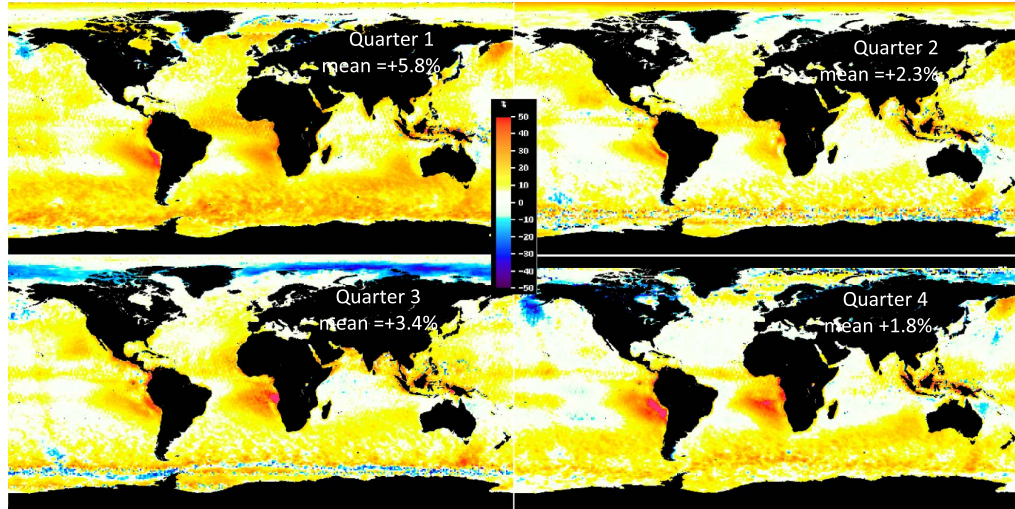


Fig. 10. Mean relative differences between MODIS Aqua and MODIS Terra noncloud fractions (or noncloud probability) for the four quarters. The relative difference is expressed as $(\text{Aqua} - \text{Terra})/\text{Aqua} \times 100\%$. A positive number means that Aqua has more cloud-free fractions (i.e., less cloud cover) than Terra.

the relatively lower cloud cover in the afternoon (Aqua) than in the morning (Terra).

For the tropical and subtropical oceans, the higher DPVOs of SST from Aqua than from Terra [see Fig. 6(c)] are consistent with the slightly higher noncloud fraction from Aqua (see Fig. 10). However, for these regions, lower DPVOs of Chl-a and nFLH from Aqua are observed [see Fig. 6(a) and (b)], suggesting that other factors may play a role. To find what led to such discrepancies, MODIS Level-2 data covering the North Indian Ocean in a typical month (January of 2006) are diagnosed, where the percentage of valid Chl-a retrievals, percentage of noncloud (i.e., not associated with the l2_flags cloud flag), percentage of straylight, and percentage of sun glint were estimated using the l2_flags.

As shown in Table II, valid Chl-a retrievals from Aqua are 15.8% less than those from Terra in the North Indian Ocean, which agrees well with the differences of noncloud observations between the two sensors. The difference of valid

TABLE II
STATISTICS OF VALID (I.E., HIGH QUALITY) CHL-A RETRIEVALS,
NONCLOUD (I.E., NOT ASSIGNED A CLOUD FLAG FROM L2_FLAGS),
STRAYLIGHT, AND HIGH SUN-GLINT OBSERVATIONS (FROM L2_FLAGS)
FROM THE MODIS LEVEL-2 PRODUCTS OVER THE NORTH INDIAN
OCEAN IN JANUARY 2006. THE LAST COLUMN SHOWS THE NONCLOUD
COVERAGE ESTIMATED USING THE MONTHLY MODIS CLOUD
FRACTION PRODUCTS (MYD08). THE RELATIVE DIFFERENCES
(RD) BETWEEN MODIS TERRA AND MODIS AQUA
ARE PROVIDED IN THE LAST ROW

| | Valid | Non-Cloud _{l2_flags} | Straylight | Sun-glint | Non-Cloud _{fraction} |
|-------|--------|-------------------------------|------------|-----------|-------------------------------|
| Terra | 12.5% | 38.1% | 32.5% | 31.4% | 38.4% |
| Aqua | 10.8% | 32.8% | 31.8% | 30.7% | 40.2% |
| RD | -15.8% | -16.3% | -2.2% | -2.3% | 4.5% |

Chl-a retrievals between Aqua and Terra during this month is also consistent with those from the climatological maps (see Fig. 2) and regional statistics [see Fig. 5(c)]. The other

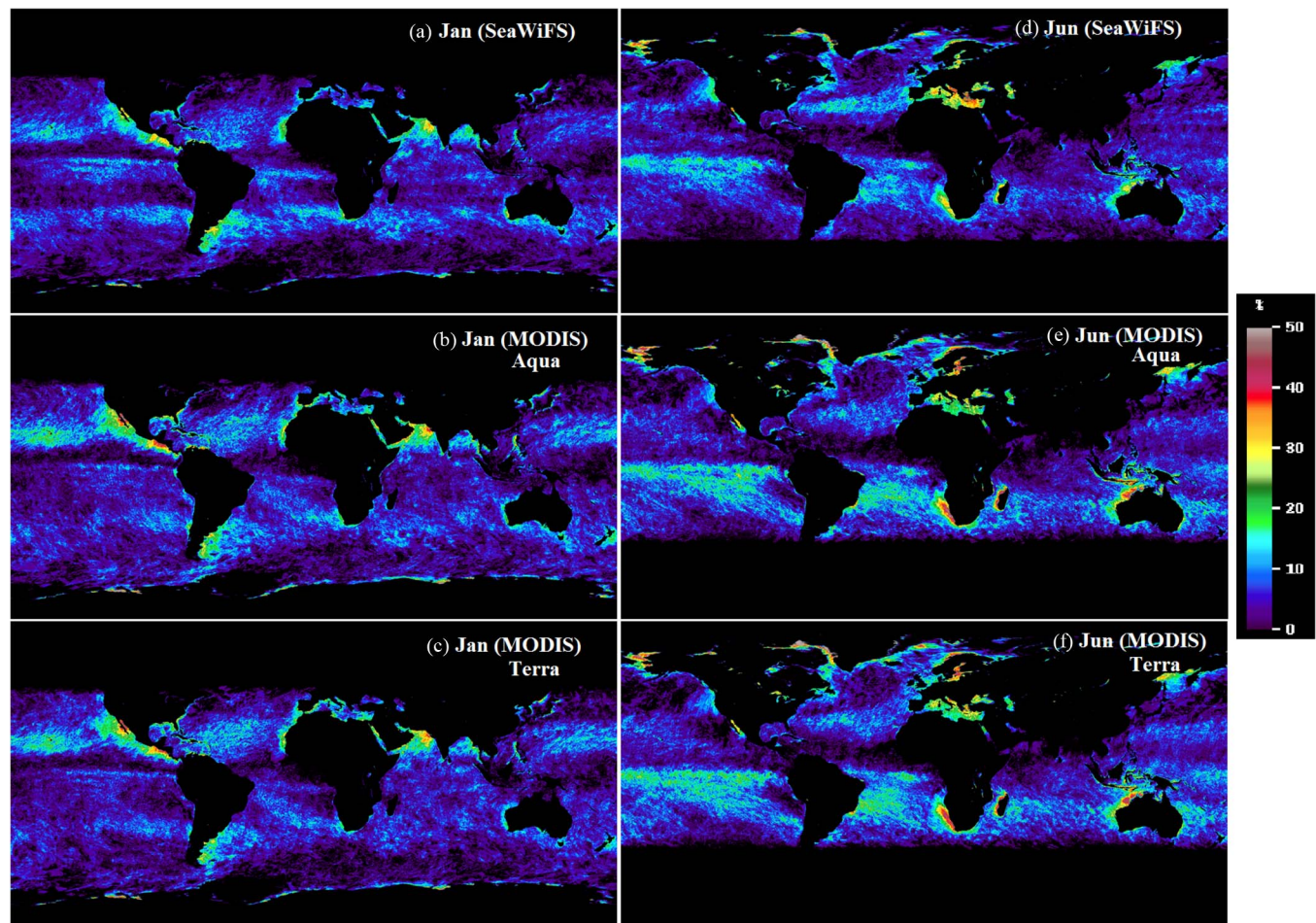


Fig. 11. Comparison of the DPVOs of Chl-a between SeaWiFS and two MODIS instruments in January and June 2003. In the tropical and subtropical oceans, higher DPVOs of SeaWiFS can be observed in the Southern Hemisphere oceans in January and in the Northern Hemisphere oceans in June due to the tilting capacity of SeaWiFS to avoid sun glint.

two quality control measures (straylight and sun glint) show very similar percentage of coverage between Aqua and Terra. However, the noncloud coverage estimated using two different methods (one from the noncloud fraction MODIS products and the other from l2_flags) show similar statistics for Terra but a large discrepancy for Aqua. This discrepancy is likely due to a misclassification of some of the sun glint pixels to clouds in the l2_flags. The single-band threshold method to discriminate clouds in l2_flags (Rayleigh-corrected reflectance after removal of the sun glint reflectance at 869 nm $> 2.7\%$) will treat some of the sun glint pixels as clouds [16]. In contrast, the MODIS cloud-fraction product is based on cloud estimates using 22 MODIS bands (standard cloud mask products) [8], which provides more realistic estimates of cloud cover.

The differences of DPVOs between Chl-a and nFLH are primarily due to their different uses of quality control flags. In addition to the flags used for Chl-a, two more flags (MODGLINT and PRODWARN) are applied to nFLH, leading to reduced nFLH DPVOs (see Fig 8). Because sun glint is more likely to affect the ocean color observations in the tropical and subtropical oceans [19], more nFLH data would be masked by the additional glint flag (see Fig. 8).

The differences of DPVOs between SST and Chl-a are primarily because SST retrievals are nearly immune to sun glint [20], leading to higher DPVOs in SST, particularly for the tropical and subtropical oceans (see Fig. 9). In addition to these regions, the Antarctic Ocean also shows higher DPVOs in SST than in Chl-a for all quarters, and the Arctic Ocean shows the same difference for Quarters 2 and 3. These may be due to the occurrence of thin cirrus clouds, which affects the l2_flags cloud mask but plays a limited role in affecting the quality of SST [10]. In contrast, if a pixel is associated with cloud or thick aerosol, the quality of Chl-a and nFLH retrievals of the pixel and the adjacency pixels can be significantly reduced [4], resulting in relatively lower DPVOs in these high-latitude regions.

B. Implications for Future Mission Design

Past ocean color sensors have been designed to have both morning and afternoon passes, with the former including the Medium Resolution Imaging Spectrometer (2002–2012) and MODIS Terra, and the latter including MODIS Aqua [1]. In the future, if a polar orbiter were to be launched, which would be preferred?

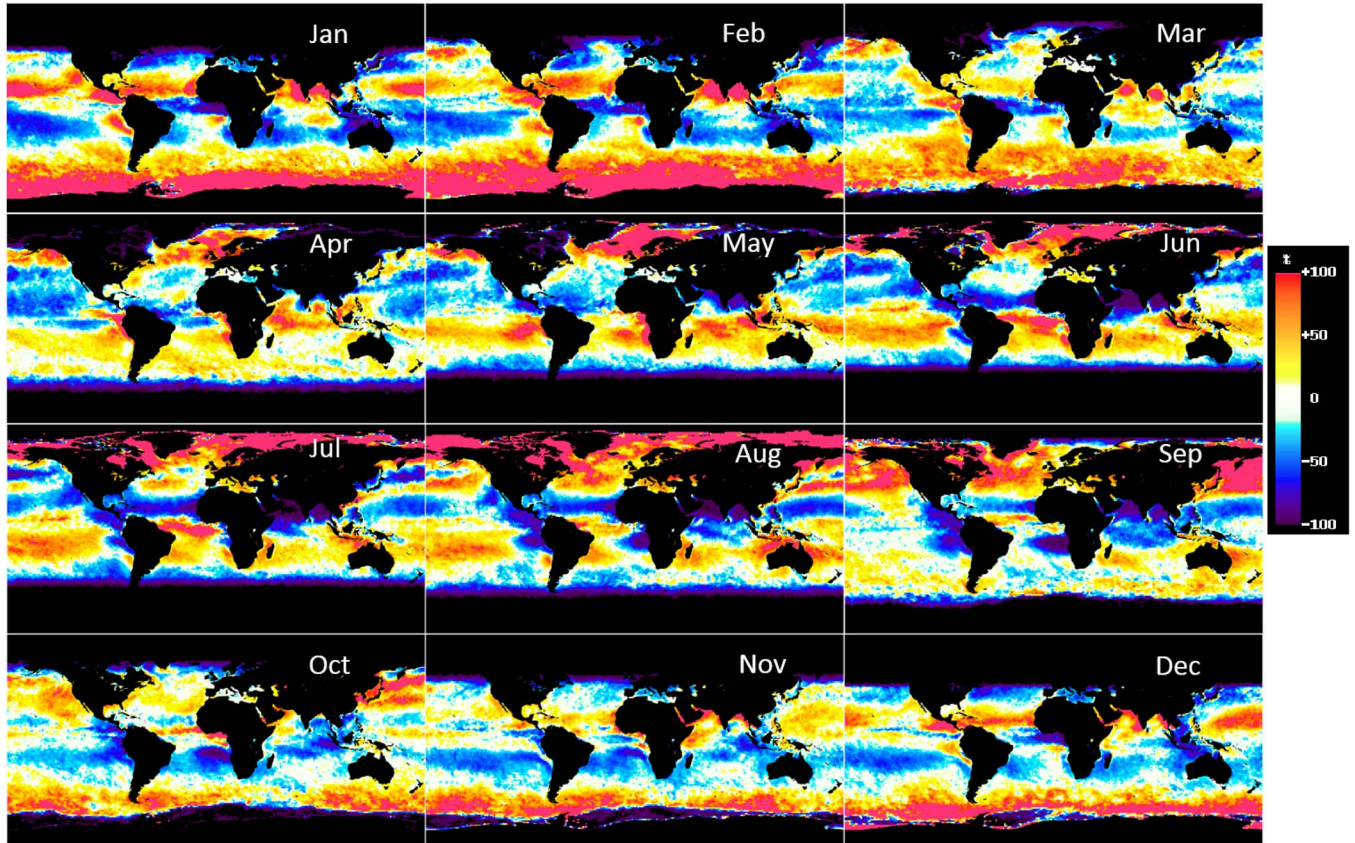


Fig. 12. Relative difference (in %) between DPVOs of each climatological month and the 12-month mean. These monthly anomalies reveal seasonality of DPVOs, which may be used to help plan field campaigns.

While the answer depends on a number of factors, in terms of percentage of valid retrievals, the findings here may give some hints.

First, for a sensor targeted for the global ocean, an afternoon pass is preferable, as more valid retrievals have been observed from Aqua than from Terra, particularly for certain regions such as the PC and AN regions and the Southern Ocean. For the global ocean, cloud coverage in the afternoon is generally lower than in the morning, and 1.8%–5.8% of more cloud-free observations (based on MOD08 and MYD08 products) can be obtained by an afternoon instrument. For a regional sensor targeted for the subtropical and tropical oceans, on the other hand, a morning pass is preferred. However, if a sensor is tilted to avoid sun glint (such as SeaWiFS, which is tilted by $\sim 22^\circ$ to either north or south), the advantage of a morning pass may disappear. For example, Fig. 11 compares the DPVOs of Chl-a between SeaWiFS and two MODIS instruments. In January 2013, most of the DPVOs between SeaWiFS and MODIS are comparable, except over the tropical and subtropical oceans in the Southern Hemisphere, a clear indication of sun glint effect. Similar observations can be made in June 2013 for the tropical and subtropical oceans in the Northern Hemisphere. Furthermore, given the large differences between DPVOs of Chl-a and nFLH and the importance of nFLH in observing phytoplankton physiology, sun glint avoidance is particularly important to increase DPVOs for nFLH, if one or more fluorescence bands are available on the sensor.

While the assessment here is on two sensors with fixed equatorial crossing times (10:30 A.M. local time for Terra and 1:30 P.M. local time for Aqua), the findings may provide some hints on planning the GEO-CAPE mission. Although the geostationary mission can, at least in theory, scan any region within its FOV multiple times a day (e.g., hourly or 3-h observations), in practice, it is impossible to perform an hourly scan on *every* region on a routine basis. The results presented here may thus help determine where, when, and how often to scan a certain region, once the information on local oceanography (e.g., bloom season) and science requirement is available.

C. Implications for Planning Field Campaigns

While the study is focused on cross-sensor differences and cross-product differences, the absolute monthly mean DPVOs can be very useful for planning field campaigns for calibrating satellite sensors and validating satellite data products, or for combining field and satellite observations to address science questions. Large field campaigns often require coordination among different groups several months (sometimes up to one year) ahead of time in order to better plan the logistics and allocate resources. Often, the coordination needs to choose a relatively narrow time window from several available ones, for example, which month is preferred if all groups can participate in October, November, and December? This certainly

depends on the local oceanography and science questions to be addressed. However, after all these factors are considered, a critical factor is the likelihood of valid retrievals. Fig. 12 shows the anomalies of DPVOs of Chl-a for MODIS Aqua during the 12 climatology months, referenced against the 12-month annual mean. These maps can be used to determine the best month (in terms of valid retrievals) for field campaigns for a particular region. For example, the likelihood to have valid retrievals over the Gulf of Mexico is much higher during winter months than during summer months. To sample the South Atlantic Bight, it is better to have a field campaign in October than in September, as the chance of obtaining valid retrievals would be much higher (at least >25%) during October.

V. CONCLUSION

Using MODIS data statistics, this paper has provided the first comprehensive analysis on the differences in the DPVOs of several ocean parameters (Chl-a, nFLH, and SST) between the two MODIS instruments on Aqua and Terra. Although the absolute DPVOs of Chl-a and nFLH are small, noticeable relative differences between the two sensors are found for different ocean regions. These findings provide valuable references for future ocean color mission design (e.g., morning or afternoon overpass) and guidance for planning field campaigns to avoid clouds and sun glint and other nonoptimal observing conditions.

ACKNOWLEDGMENT

The authors would like to thank NASA OBPG, who has provided all satellite data for this analysis. They would also like to thank the two anonymous reviewers for providing valuable comments to help improve this paper.

REFERENCES

- [1] C. R. McClain, "A decade of satellite ocean color observations," *Annu. Rev. Marine Sci.*, vol. 1, pp. 19–42, Jan. 2009.
- [2] B. B. Barnes and C. Hu, "Cross-sensor continuity of satellite-derived water clarity in the gulf of Mexico: Insights into temporal aliasing and implications for long-term water clarity assessment," *IEEE Trans. Geosci. Remote Sens.*, vol. 53, no. 4, pp. 1761–1772, Apr. 2015.
- [3] M. Wang *et al.*, "Impacts of VIIRS SDR performance on ocean color products," *J. Geophys. Res., Atmos.*, vol. 118, no. 18, pp. 10 347–10 360, Sep. 2013.
- [4] R. A. Barnes *et al.*, "SeaWiFS technical report series," Volume 23: SeaWiFS prelaunch radiometric calibration and spectral characterization, NASA Goddard Space Flight Center, Greenbelt, MD, USA, NASA Tech. Memo. 104566, 1994.
- [5] S. Maritorena, O. H. F. d'Andon, A. Mangin, and D. A. Siegel, "Merged satellite ocean color data products using a bio-optical model: Characteristics, benefits and issues," *Remote Sens. Environ.*, vol. 114, no. 8, pp. 1791–1804, Aug. 2010.
- [6] J.-K. Choi *et al.*, "GOFCI, the world's first geostationary ocean color observation satellite, for the monitoring of temporal variability in coastal water turbidity," *J. Geophys. Res., Oceans*, vol. 117, no. C9, Sep. 2012, Art. ID C9004.
- [7] J. Fishman *et al.*, "The United States' next generation of atmospheric composition and coastal ecosystem measurements: NASA's Geostationary Coastal and Air Pollution Events (GEO-CAPE) Mission," *Bull. Amer. Meteorol. Soc.*, vol. 93, no. 10, pp. 1547–1566, Oct. 2012.
- [8] S. Platnick *et al.*, "The MODIS cloud products: Algorithms and examples from Terra," *IEEE Trans. Geosci. Remote Sens.*, vol. 41, no. 2, pp. 459–473, Feb. 2003.
- [9] M. D. King, S. Platnick, W. P. Menzel, S. A. Ackerman, and P. A. Hubanks, "Spatial and temporal distribution of clouds observed by MODIS onboard the Terra and Aqua satellites," *IEEE Trans. Geosci. Remote Sens.*, vol. 51, no. 7, pp. 3826–3852, Jul. 2013.
- [10] R. Holz *et al.*, "Global Moderate Resolution Imaging Spectroradiometer (MODIS) cloud detection and height evaluation using CALIOP," *J. Geophys. Res.*, vol. 113, no. D8, Apr. 2008, Art. ID D00A19.
- [11] W. P. Menzel and J. F. W. Purdom, "Introducing GOES-I: The first of a new generation of geostationary operational environmental satellites," *Bull. Amer. Meteorol. Soc.*, vol. 75, no. 5, pp. 757–781, May 1994.
- [12] M. Wang and S. W. Bailey, "Correction of sun glint contamination on the SeaWiFS ocean and atmosphere products," *Appl. Opt.*, vol. 40, no. 27, pp. 4790–4798, Sep. 2001.
- [13] M. J. Behrenfeld *et al.*, "Satellite-detected fluorescence reveals global physiology of ocean phytoplankton," *Biogeosciences*, vol. 6, no. 5, pp. 779–794, May 2009.
- [14] C. Hu, B. B. Barnes, L. Qi, and A. A. Corcoran, "A harmful Algal bloom of Karenia brevis in the Northeastern Gulf of Mexico as revealed by MODIS and VIIRS: A comparison," *Sensors*, vol. 15, no. 2, pp. 2873–2887, Jan. 2015.
- [15] C. Hu *et al.*, "Red tide detection and tracing using MODIS fluorescence data: A regional example in SW Florida coastal waters," *Remote Sens. Environ.*, vol. 97, no. 3, pp. 311–321, Aug. 2005.
- [16] S. Hooker *et al.*, "Algorithm updates for the fourth SeaWiFS data reprocessing," NASA Goddard Space Flight Center, Greenbelt, MD, USA, NASA Tech. Memo. 2003-206892, 2003.
- [17] J. G. Acker and G. Leptoukh, "Online analysis enhances use of NASA Earth science data," *EOS, Trans. Amer. Geophys. Union*, vol. 88, no. 2, pp. 14–17, Jan. 2007.
- [18] S. Hill and Y. Ming, "Nonlinear climate response to regional brightening of tropical marine stratocumulus," *Geophys. Res. Lett.*, vol. 39, no. 15, Aug. 2012, Art. ID L15707.
- [19] W. W. Gregg and M. E. Conkright, "Global seasonal climatologies of ocean chlorophyll: Blending in situ and satellite data for the coastal zone color scanner era," *J. Geophys. Res., Oceans*, vol. 106, no. C2, pp. 2499–2515, Feb. 2001.
- [20] I. Khalil, C. Mannaerts, and W. Ambarwulan, "Distribution of chlorophyll-a and sea surface temperature (SST) using MODIS data in east Kalimantan waters, Indonesia," *J. Sustainability Sci. Manage.*, vol. 4, pp. 113–124, 2009.



Lian Feng received the Ph.D. degree in cartography and geography information system from Wuhan University, Wuhan, China, in 2013.

His research interests include remote sensing of inland and coastal water environments and how these environments are influenced by climate variability and human activities. He is currently a Postdoctoral Associate with the Optical Oceanography Laboratory, College of Marine Science, University of South Florida, Tampa, FL, USA.



Chuanmin Hu received the B.S. degree in physics from the University of Science and Technology of China, Hefei, China, in 1989 and the Ph.D. degree in physics (ocean optics) from the University of Miami, Coral Gables, FL, USA, in 1997.

He is currently a Professor with the College of Marine Science, University of South Florida, St. Petersburg, FL, where he is also the Director of the Optical Oceanography Laboratory. He has been a Principal or a Coprincipal Investigator of several projects funded by the U.S. National Aeronautics and Space Administration, the National Oceanic and Atmospheric Administration, the Environmental Protection Agency, and the U.S. Geological Survey to study river plumes, red tides, water quality and benthic habitat health, and connectivity of various ecosystems.